Journal of Morphology

IMMUNOHISTOCHEMICAL PROFILING OF THE ULTIMOBRANCHIAL REMNANTS IN THE RAT POSTNATAL THYROID GLAND

Journal:	*Journal of Morphology*
Manuscript ID	Draft
Wiley - Manuscript type:	Research Article
Date Submitted by the Author:	n/a
Complete List of Authors:	Vázquez-Román, Victoria; Medicine School. University of Seville. , Cytology and Histology Utrilla, José; Medicine School. University of Seville, Citology and Histology Fernández-Santos, José; Medicine School. University of Seville, Citology and Histology Martín-Lacave, Inés; Medicine School. University of Seville, Cytology and Histology
Keywords:	ultimobranchial follicle (UBF), immunohistochemistry (IHC), rat thyroid

IMMUNOHISTOCHEMICAL PROFILING OF THE ULTIMOBRANCHIAL REMNANTS IN THE RAT POSTNATAL THYROID GLAND

Victoria Vázquez-Román*, José C. Utrilla*, José M. Fernández-Santos and Inés Martín-Lacave.

Department of Normal and Pathological Cytology and Histology, School of Medicine, University of Seville, Spain.

Short Title: Immunohistochemistry of ultimobranchial remnants in rat thyroid

* Victoria Vázquez-Román and José C. Utrilla contributed equally to this work.

Corresponding author:

Inés Martín-Lacave

Dpt. Normal and Pathological Cytology and Histology

School of Medicine

Avda. Sánchez-Pizjuán s/n

41009 Seville, Spain.

Email: ilacave@us.es

ABSTRACT

Ultimobranchial (UB) remnants are a constant presence in the thyroid throughout rat postnatal life; however, the difficulty in identifying the most immature forms from the surrounding thyroid tissue prompted us to search for a specific marker. With that objective, we applied a panel of antibodies reported to be specific for their human counterpart, solid cell nests (SCNs), using double immunohistochemistry and immunofluorescence. Our results demonstrated that cytokeratin 34βE12 and p63 are highly sensitive markers for the immunohistologic screening of UB remnants, independently of their maturity or size. Furthermore, rat UB follicles (UBFs) coincided with human SCNs in the immunohistochemical pattern exhibited by both antigens. In contrast, the pattern displayed for calcitonin and thyroglobulin differs considerably but is compatible with the hypothesis that UB cells can differentiate into both types of thyroid endocrine cells. This hypothesis agrees with recent findings that thyroid C cells share an endodermic origin with follicular cells in rodents. We suggest that the persistence of p63-positive undifferentiated cells in UB remnants may constitute a reservoir of basal/stem cells that persist beyond embryogenesis from which, in certain unknown conditions, differentiated thyroid cells or even unusual tumours may arise.

Keywords: ultimobranchial follicle (UBF), immunohistochemistry (IHC), rat thyroid.

INTRODUCTION

In mammals, the thyroid gland consists of two endocrine cell populations, follicular cells and C cells, with different functions and embryonic origins. During development, the thyroid diverticulum, which is derived from the ventral pharyngeal floor, moves caudally along the midline and forms two lateral lobes, thus giving rise to follicular cells. In parallel, the two UB bodies (UBBs) are separated from the last pair of pharyngeal pouches and approach the thyroid vesicle until their fusion, becoming embedded in the thyroid lobes and giving rise to C cells (Fagman and Nilsson, 2011; Westerlund et al., 2008). In contrast, in lower vertebrates, such as birds and fishes, no fusion of the UBBs with the thyroid lobes occurs, but they remain as separate glands called UB glands; hence, the thyroid gland is exclusively composed of follicular cells (Fagman and Nilsson, 2010).

The UBBs, apart from forming C cells, remain in the adult thyroid gland as rather complex structures considered as embryonic remnants with unknown significance. These structures show differences among species and have been described in the literature under different names. Specifically, they have been extensively studied in rats, where they are mostly known as "ultimobranchial follicles" (UBFs) (Martin-Lacave et al., 1992; Rao-Rupanagudi et al., 1992; Van Dyke, 1944; Wollman and Neve, 1971a; b) and in humans, where they are termed "solid cell nests" (SCNs) (Beckner et al., 1990; Harach, 1988; Harach et al., 1993).

It is generally accepted that both UBFs in rats and SCNs in humans are embryonic remnants of UBBs and, therefore, share a common origin (Bellevicine et al., 2012; Wollman and Hilfer, 1977; 1978). Nevertheless, despite this common embryonic origin, there are differences regarding the appearance and evolution of these UB remnants

during postnatal life in both species. Specifically, in rats, these structures appear in all the thyroid glands, although they adopt different morphological patterns throughout postnatal life (Vazquez-Roman et al., 2013). Thus, in young rats (0-180 days), they evolve from narrow cellular nests to tubular forms, the so-called "immature UBFs". In addition, "mixed follicles", which are partially formed by UBFs fusing to usual thyroid follicles, may also be observed in young rats. In contrast, in adult rats (6-15 months) and old rats (18-24 months), mature cystic forms predominate, the so-called "mature UBFs", which are rather rounded, with stratified flattened cells in the wall, and cellular debris in the lumen. Moreover, in adult and old rats, an unusual progression of the forms described above can be found that resembles enormous onion-like structures that we have termed "UB cystoadenomata". With the exception of UB cystoadenomata, there are difficulties in the microscopic identification of UB remnants from the surrounding parenchyma due to either relative small size or their uncharacteristic form (Vazquez-Roman et al., 2013).

In humans, diverse immunohistochemical (IHC) studies have been performed to characterize the cellular composition of SCNs (Burstein et al., 2004; Cameselle-Teijeiro et al., 1994; Mizukami et al., 1994; Preto et al., 2004; Reis-Filho et al., 2003; Rios Moreno et al., 2011). According to those studies, two cell types form the SCNs, which are referred to as "main cells" and "C cells". Specifically, "main cells" can be immunostained for some cytokeratins (CK34βE12, CK7, CK11, CK19, carcinoembryonic antigen (CEA), galectina-3, as well as different markers expressed in the basal/stem cells of stratified epithelium, such as p63, bcl-2 or telomerase. In contrast, C cells are positive for calcitonin (CT), calcitonin gene-related peptide

(CGRP), chromogranin and thyroid transcription factor (TTF-1), but lack immunoreactivity for p63.

In rats, no IHC studies on UBFs have been reported, with the exception of two articles published by us in which the occasional presence of CT and thyroglobulin (Tg) in the wall was analysed (Conde et al., 1992; Vazquez-Roman et al., 2013). No published data describe a precise staining method to specifically identify UBFs in the rat independently of their morphological pattern and magnitude. In addition, there are no specific IHC analyses that could help to clarify their cellular composition and whether the UBFs are homogeneous structures composed only of "U-cells", as stated by Wollman and Neve (Wollman and Neve, 1971a; b), or if they are rather heterogenic structures, such as SCNs (Cameselle-Teijeiro et al., 1994; Harach, 1988; Martin et al., 2000). Furthermore, no new evidence has been provided to clarify whether UB remnants contribute to the formation of C cells and thyroid follicular cells during postnatal life in mammals, and their possible contribution to certain types of pathology at the thyroid level remains to be elucidated. Therefore, the main objectives of the present article were addressed to shed light on the aforementioned aspects.

MATERIALS AND METHODS

Selection of samples

The study material consisted of sixty formalin-fixed, paraffin-embedded and serially sectioned thyroid glands of Wistar rats, of both sexes and different ages, in which we previously described the appearance of different morphological patterns that adopt the UB remnants throughout rat postnatal life (Vazquez-Roman et al., 2013). Specifically, 25 cases of "immature UBFs" (detected in young rats), 25 cases of "mature UBFs" (detected in adult rats), and 10 cases of UB cystadenomata (detected in old rats) were analysed. All experiments were conducted in accordance with the guidelines proposed in The Declaration of Helsinki (http://www.wma.net) involving the use of laboratory animals.

Immunohistochemical Analysis

Single Immunohistochemistry

Once a particular UBF pattern was detected in a thyroid section, consecutive sections of the same thyroid gland were selected to proceed with the IHC study. Silane-coated sections were dewaxed in xylene and hydrated through graded alcohols. Next, an antigen retrieval step using EnVision Flex Target Retrieval High pH (DAKO, Denmark) was performed in a heating instrument, PTLink (DAKO), at 96ºC for 20 min, according to the manufacturer's instructions. The slides were immersed in a washing solution (Wash Buffer DAKO) for 5 min. Then, the sections were treated with 3% hydrogen peroxide to block endogenous peroxidase activity for 20 min. The slides were then incubated with a panel of primary antibodies (see Table 1), at 4 °C overnight in a humidified chamber. EnVision Flex/HRP (DAKO) was used as the labelling system according to the manufacturer's instructions, and 3,3'-diaminobenzidine

tetrahydrochloride (DAB) solution (Sigma–Aldrich, Germany) was used as chromogen. The slides were counterstained with haematoxylin, dehydrated and coverslipped. Photomicrographs of the samples were performed using an Olympus photomicroscope (Vanox AHBT3).

Double Immunohistochemistry

To analyse the colocalization of CT or Tg with p63, double IHC labelling was performed with an antigen retrieval step in between the two staining sequences to prevent cross-reactions among reagents, according to Lan et al. (Lan et al., 1995). Briefly, the sections were dewaxed and pretreated in the same manner as described above for single IHC but without the antigen retrieval step. In the first immunostaining sequence, the specific antibody (anti-CT or anti-Tg) was incubated at 4 ºC overnight and followed either by the LSAB/Alkaline Phosphatase system (DAKO), for CT, or EnVision Flex, for Tg. The enzymatic reaction was visualized with Fast Red or DAB-Cobalt-chloride (Sigma–Aldrich) as chromogens, respectively. Next, an antigen retrieval step using EnVision Flex Target Retrieval High pH, as described above, was intercalated before the second immunostaining sequence started. The second specific antibody, anti-p63, was incubated at 4 ºC overnight, and EnVision Flex/HRP or LSAB/Alkaline Phosphatase (DAKO) were used as the labelling systems. After colour development with DAB or DAB-Cobalt-chloride as chromogens, the slides were counterstained with haematoxylin and coverslipped in an aqueous permanent medium.

To analyse the colocalization of TTF-1 with CK34βE12, a similar technique was used but before applying the first specific antibody (anti-TTF-1) an antigen retrieval step with EDTA buffer, pH 9 (DAKO, Denmark) was carried out. The specific binding was developed using streptavidin-biotin-peroxidase technique (LSAB+/HRP kit, DAKO),

and DAB (Sigma–Aldrich, Germany) as chromogen. In the second immunostaining sequence, the specific antibody (anti-CK34βE12) was incubated at 4 ºC overnight, followed by the LSAB/Alkaline Phosphatase system (DAKO) and enzymatic development with Fast-Red as chromogen.

Double Immunofluorescence (IF)

To analyse the colocalization of p63 or CK34βE12 with CT or Tg, respectively, by double IF, thyroid sections were dewaxed, hydrated and pretreated for antigen retrieval using Target Retrieval High pH buffer, as described above. Nonspecific binding was blocked with 10% normal donkey serum for 15 min (Jackson ImmunoResearch Laboratories). Then, the monoclonal primary antibody, either p63 or CK34βE12, was added for 1 h at room temperature in a humidified chamber. Subsequently, the slides were washed and incubated with Cy3-labeled donkey anti-mouse IgG secondary antibody (1:100, Jackson ImmunoResearch Laboratories) for 30 min at room temperature in a humidified chamber. After washing in PBS, the second immunostaining sequence started. The slides were then incubated with a specific polyclonal anti-CT antibody or anti-Tg antibody and, subsequently, with Cy2-labeled donkey anti-rabbit IgG antibody (1:100, Jackson ImmunoResearch Laboratories) under the same conditions as before. After washing in PBS, DAPI (Sigma-Aldrich) was added for nuclear counterstaining, and the slides were coverslipped with antifading mounting medium (Mowiol 4-88, Sigma-Aldrich). The sections were visualized with a fluorescence microscope (Olympus BX50, Hamburg, Germany). Images were acquired using an ORCA-03G digital camera (Hamamatsu, Bridgewater, Rockville, USA) and analysed using Image PRO-PLUS 7.0 software (Media Cybernetics, USA). The antigen combinations were as follows: p63-CT, p63-Tg, CK34βE12-CT, and CK34βE12-Tg.

Controls for immunostaining specificity consisted of: (i) omitting any essential step of the immunoreaction and (ii) replacing the primary antibody with an appropriate dilution of mouse or rabbit IgG serum (Sigma-Aldrich), followed by the IHC or IF protocol as outlined above. For p63 and TTF-1, only nuclear immunoreactivity was considered specific, while for all other markers only cytoplasmic staining was accepted.

RESULTS

In general, UBFs are located in the centre of the thyroid lobe, intimately related with the adjacent thyroid parenchyma and frequently in contact with perivascular connective tissue. The centre of the thyroid lobe is also the area in which C cells are more numerous, the so-called "C-cell area". The results of the IHC study of UB remnants are summarized in Table 2.

Cytokeratins (CKs)

CKs AE1/AE3 and 34βE12 consistently decorated all forms of UB remnants and displayed different IHC patterns. Specifically, CKAE1/AE3 stained UBFs as well as follicular and C cells in adjacent thyroid tissue. UBF immunostaining was rather homogeneous, independently of whether they were immature cell aggregates, mature cystic UBFs or cystoadenomata (Fig. 1 A1, B1, C1). In contrast, CK34βE12 immunostaining was exclusively restricted to the UB remnants. Specifically, immature solid forms of UBFs were strongly stained for CK34βE12; even small cell aggregates of as few as 3 to 10 cells intermingled among the background thyroid follicles could be perfectly distinguished (Fig. 1 A2). In mature cystic UBFs, as well as in cystoadenomata, the immunostaining for CK34βE12 was only detected in the cellular wall, but staining was negative in the desquamative material of the lumen (Fig. 1 B2, C2).

p63

p63 was intensely expressed in all UBFs but was not detected in any cell of the adjacent thyroid tissue. The pattern of p63 immunostaining varied depending on the maturity of the UBF throughout postnatal life. In small cellular nests, all UB cells apparently exhibited a strong nuclear staining of p63 (Fig. 1 A3); however, whenever a cystic

structure appeared, as occurs in both mature UBFs (Fig. 1 B3) and cystadenomata (Fig.1 C3), the immunostaining of p63 was compartmentalized, with strong positivity of peripheral basal undifferentiated cells and nonstaining of centrally located squamous cells.

Consequently, both CK34βE12 and p63 are the most useful markers for the immunohistologic screening of UB remnants in the rat thyroid. Even at a low-power magnification, cytokeratin 34βE12 and p63 immunoreactivities were easily detectable and restricted to UBFs, in which they were concomitantly expressed.

TTF-1/Nkx2.1

Positive staining for TTF-1 was present in all differentiated cells of the adjacent thyroid parenchyma (follicular cells and C cells), but UBFs were mainly negative, independently of their grade of maturity, except for a few cells that appeared in the wall of some UBFs (Fig. 1 A4, B4) and in mixed follicles. Cystadenomata were negative (Fig. 1 C4).

Calcitonin and thyroglobulin

CT immunostaining was detected in the C cells of the surrounding thyroid tissue as expected, but not in UBFs, with the exception of a few isolated positive cells distributed at the periphery of the wall of a pair of UBFs. In relation to Tg immunostaining, most UBFs were negative. Nevertheless, some immunostaining could be observed in scattered cells, the colloid-like material that is characteristic of some immature UBFs, and mixed follicles.

Double IHC and double IF

To analyse the precise localization of antigens of terminal thyroid differentiation, such as CT and Tg, in the UBF wall, double IHC and double IF were performed. Specifically, for double IHC studies, the colocalization of CT or Tg, which share a cytoplasmatic pattern, was combined with p63, the nuclear IHC-specific marker of UBFs. As shown in Figure 2, CT-positive cells were not particularly more abundant in the thyroid tissue that surrounded UBFs. Furthermore, UBFs were generally negative for CT, with the exception of scarce immature UBFs that were detected in few-day-old rats, which presented immunostaining for CT in sporadic C cells located at the periphery (Fig. 2 A). In contrast, when Tg and p63 were colocalized in immature UBFs by double IHC, a rather more complex pattern was observed. Thus, some immunoreactivity for Tg was displayed at the cytoplasmic level in scarce p63-negative cells as well as in some colloid-like drops that appeared within the UBF wall (Fig. 3 A) Furthermore, Tg was also observed in the lumen of mixed follicles emerging from the UBF wall (Fig. 3 B). Conversely, mature UBFs and cystadenomata were consistently negative.

When double IF was used instead, the results obtained at the thyroid level were strikingly clearer than those obtained by double IHC; however, they did not differ from the findings described above. UBFs were strongly labelled using either p63 or cytokeratin 34βE12 antibodies, independently of the type of UBF or the age of the rat (Figs. 4 and 5). The colocalization of these markers with CT or Tg perfectly distinguished the UBF, which was strongly immunostained for p63 or CK34βE12, and the surrounding thyroid tissue, which was completely negative for those markers but immunopositive for either CT (Fig. 4) or Tg (Fig. 5). Furthermore, in the wall of immature UBFs, several cell types could be distinguished according to their

immunostaining pattern and localization: (1) undifferentiated UB cells exclusively positive for p63 or CK34βE12 and mainly confined to the periphery; (2) epithelial squamous cells negative for those antigens and centrally located in a developing lumen; and (3) a few thyroid differentiated cells positive for either Tg or, much less frequently, CT (Figs. 4 and 5). In contrast, in mature UBFs and cystoadenomata, only undifferentiated UB cells and epithelial squamous cells were observed.

Nevertheless, when Tg immunostaining was displayed by some immature UBFs, it was difficult to determine whether the immunopositive cells or the colloid-like material were components of the UBF itself or normally existing thyroid follicles entrapped by the growing UB remnants (Fig. 5B).

Finally, we analysed the co-expression of TTF1 (nuclear antigen of thyroid differentiation) with CK34βE12 in the UBF wall using double IHC (Fig. 6). Although most thyroid cells were positive, UBFs were mainly negative, with the exception of some TTF1-positive scattered cells found in the most immature UBFs, which could also express (Fig. 6C) or not express CK (Fig. 6B).

DISCUSSION

We have recently demonstrated that despite previous controversy (Rao-Rupanagudi et al., 1992; Takaoka et al., 1995), UB remnants are a constant presence in the thyroid throughout rat postnatal life (Vazquez-Roman et al., 2013). However, the difficulty in identifying the most immature forms from the surrounding thyroid tissue led us to search for a specific marker of UBFs, independently of their maturity or size. With that objective, we have applied several antibodies reported to be specific of their human counterpart, SCNs, including different types of keratins and p63 (Burstein et al., 2004; Cameselle-Teijeiro et al., 2005a; Harach and Wasenius, 1987; Mizukami et al., 1994; Reis-Filho et al., 2003; Rios Moreno et al., 2011). According to our results, all types of rat UB remnants – either solid or cystic immature forms, mature UBFs or cystadenomata – were without exception positive for both CK34βE12 and p63 at any age of the animal. Even the most immature UBFs, sometimes composed of only as few as 3-10 cells, were strikingly apparent against the negativity of the rest of the thyroid components. Therefore, we can affirm that either CK34βE12 or p63 are highly sensitive markers for the immunohistologic screening of UB remnants.

Furthermore, both rat UBFs and human SCNs, in addition to sharing CK34βE12 and p63 as specific staining markers, coincided in the IHC pattern exhibited by both antigens. Specifically, solid immature forms of UBFs displayed uniform strong staining in all cells, which were apparently undifferentiated; these cells are the so-called “U cells” in rat UBFs (Neve and Wollman, 1971; Wollman and Hilfer, 1978) or “main cells” in SCNs (Cameselle-Teijeiro et al., 2005b; Cameselle-Teijeiro et al., 1994; Reis-Filho et al., 2003; Rios Moreno et al., 2011). However, when epithelial squamoid differentiation appeared in the cystic UBFs, the immunopositivity was restricted to the

most peripheral cells, as it also occurs in different forms of SCNs (Reis-Filho et al. 2003; Burstein et al. 2004). In contrast, the patterns displayed for CT and Tg differed considerably between both types of UB remnants. In rats, CT-positive cells were only found in very scarce immature UBFs or in the walls of UBFs presenting aberrant localization at the thyroid level, as we previously reported (Martin-Lacave et al. 1992). Furthermore, no increase in the number of C cells was found in the background thyroid tissue near the UB remnants. Therefore, we conclude that UBFs do not normally contribute to the formation of new C cells during rat postnatal life, which is the opposite to that observed in humans in which numerous C cells are intermingled with main cells in SCNs (Cameselle-Teijeiro et al., 2005b; Harach and Wasenius, 1987; Mizukami et al., 1994; Reis-Filho et al., 2003; Rios Moreno et al., 2011). Nevertheless, the capacity, if any, of those postnatal C cells to migrate from UB remnants along the connective tissue to occupy their definitive position in relation to thyroid follicles, likely through an epithelial mesenchymal transition process (EMT) (Acloque et al., 2009), remain to be elucidated.

Some differences were found between UBFs and SCNs in relation to their IHC pattern for Tg. Specifically, Tg was observed at the cytoplasmic level in scarce p63-negative cells as well as in some colloid-like drops that appeared within the wall of immature UBFs. Conversely, in humans, no Tg-positive cells have ever been reported as forming a part of SCNs (Autelitano et al., 1987; Cameselle-Teijeiro et al., 2005b; Cameselle-Teijeiro et al., 1994; Mizukami et al., 1994; Reis-Filho et al., 2003; Rios Moreno et al., 2011). Accordingly, we also observed scarce cells expressing TTF-1, a common marker of differentiated thyroid cells, either follicular cells (Lazzaro et al., 1991) or C cells

(Suzuki et al., 1998), in the UBF wall. This finding is compatible with the hypothesis that UB cells could differentiate into both endocrine cell populations, as we previously suggested (Martin-Lacave et al., 1992; Moreno et al., 1989). This hypothesis agrees with the findings of Kameda and cols. (Kameda et al., 2007) who discarded that mammalian thyroid C cells are derived from the neural crest, as it occurs with avian CT-producing cells of the UB gland (Kameda, 1995). The authors demonstrated by fate mapping of neural crest cells in both Wnt1-Cre/R26R and Connexin (Cxn) 43-lacZ transgenic mice that neural crest cells did not colonize the fourth pharyngeal pouch or the UBB (Kameda, 2016; Kameda et al., 2007). Furthermore, Johansson et al. have recently clarified using lineage tracing in Sox17-2A-iCre/R26R mice that pharyngeal endoderm-derived cells give rise to C cells (Johansson et al., 2015). Both findings together indicate that mouse thyroid C cells are derived from the endodermal epithelial cells of the fourth pharyngeal pouch; hence, they share an endodermic origin with follicular cells, which are derived from the ventral pharyngeal floor. Therefore, the present data are compatible with the hypothesis that the foregut endoderm gives rise to both thyroid endocrine cell types in the rat, as previously proposed by Westerlund et al. for the mouse (Westerlund et al., 2008).

Based on the fact that all normal rat thyroid glands have UBFs throughout adult life, a question arises about the meaning of the persistence of the UB remnants. The same question was raised by Ozaki et al. for human SCNs (Ozaki et al., 2011). We agree with those authors that the answer to this question is likely related to the constant presence of undifferentiated cells associated with UB remnants in mammals, independently of their own peculiarities. The existence of p63-positive cells suggests that they may constitute a reservoir of basal/stem cells that persists beyond embryogenesis from which, in

certain unknown conditions, differentiated thyroid cells or even unusual tumours, such as rat UB cystoadenomata (Vazquez-Roman et al., 2013), human mucoepidermoid (Cameselle-Teijeiro et al., 1994; Harach et al., 1993) or mixed medullary and follicular carcinomas (Matias-Guiu, 1999), may arise. Moreover, Ozaki et al. (Ozaki et al., 2012) recently demonstrated the appearance of numerous clear immature cells after partial thyroidectomy that expressed keratin14 and Foxa2, the definitive endoderm lineage marker; these cells could be derived from the UBB, suggesting a critical role for UB remnants in thyroid regeneration (Okamoto et al., 2013).

There is evidence for the presence of adult stem cells of endodermic origin in the human thyroid gland that express OCT4, a classical marker of stem cells (Thomas et al., 2006). Stem cells, ranging from 0.3%-1.4% of the total cell population, were also obtained from mouse thyroid glands; half of the cells expressed OCT4 in addition to other specific stem cell markers, such as ABCG2 and nucleostatin (Hoshi et al., 2007). It has repeatedly been proposed that SCNs may represent a pool of stem cells that could contribute to the histogenesis of thyroid cells and thyroid regeneration in adult life (Preto et al., 2004; Reis-Filho et al., 2003). According to our results, the same could be suggested for UB remnants in the rat thyroid gland. Nevertheless, further studies are required to understand the true nature of undifferentiated UB cells and their relationship to differentiated thyroid cells throughout postembryonic life.

AUTHOR CONTRIBUTIONS

VVR: acquisition of data, data analysis and interpretation. JCU: modified the methodology, acquisition of data, data analysis and interpretation. JFS: artwork,

manuscript revisión and approval. IML: concept and design of the study, wrote the manuscript. Neither author has any conflict of interest to declare.

ACKNOWLEDGEMENTS

This work was supported by grants from the Consejería de Innovación, Ciencia y Empresa (refs. CTS-439/2011), and from the Consejería de Salud (ref. PI-0051-2013), Junta de Andalucía, Spain. The authors thank Mr. John Brown for English language corrections.

REFERENCES

Acloque H, Adams MS, Fishwick K, Bronner-Fraser M, Nieto MA. 2009. Epithelial-mesenchymal transitions: the importance of changing cell state in development and disease. J Clin Invest 119(6):1438-1449.

Autelitano F, Santeusanio G, Di Tondo U, Costantino AM, Renda F, Autelitano M. 1987. Immunohistochemical study of solid cell nests of the thyroid gland found from an autopsy study. Cancer 59(3):477-483.

Beckner ME, Shultz JJ, Richardson T. 1990. Solid and cystic ultimobranchial body remnants in the thyroid. Arch Pathol Lab Med 114(10):1049-1052.

Bellevicine C, Ippolito S, Arpaia D, Ciancia G, Pettinato G, Troncone G, Biondi B. 2012. Ultimobranchial body remnants (solid cell nests) as a pitfall in thyroid pathology. J Clin Endocrinol Metab 97(7):2209-2210.

Burstein DE, Nagi C, Wang BY, Unger P. 2004. Immunohistochemical detection of p53 homolog p63 in solid cell nests, papillary thyroid carcinoma, and hashimoto's thyroiditis: A stem cell hypothesis of papillary carcinoma oncogenesis. Hum Pathol 35(4):465-473.

Cameselle-Teijeiro J, Abdulkader I, Soares P, Alfonsin-Barreiro N, Moldes-Boullosa J, Sobrinho-Simoes M. 2005a. Cystic tumor of the atrioventricular node of the heart appears to be the heart equivalent of the solid cell nests (ultimobranchial rests) of the thyroid. Am J Clin Pathol 123(3):369-375.

Cameselle-Teijeiro J, Preto A, Soares P, Sobrinho-Simoes M. 2005b. A stem cell role for thyroid solid cell nests. Hum Pathol 36(5):590-591.

Cameselle-Teijeiro J, Varela-Duran J, Sambade C, Villanueva JP, Varela-Nunez R, Sobrinho-Simoes M. 1994. Solid cell nests of the thyroid: light microscopy and immunohistochemical profile. Hum Pathol 25(7):684-693.

Conde E, Moreno AM, Martin-Lacave I, Fernandez A, Galera H. 1992. Immunocytochemical study of the ultimobranchial tubule in Wistar rats. Anat Histol Embryol 21(1):94-100.

Fagman H, Nilsson M. 2010. Morphogenesis of the thyroid gland. Mol Cell Endocrinol 323(1):35-54.

Fagman H, Nilsson M. 2011. Morphogenetics of early thyroid development. J Mol Endocrinol 46(1):R33-42.

Harach HR. 1988. Solid cell nests of the thyroid. J Pathol 155(3):191-200.

Harach HR, Vujanic GM, Jasani B. 1993. Ultimobranchial body nests in human fetal thyroid: an autopsy, histological, and immunohistochemical study in relation to solid cell nests and mucoepidermoid carcinoma of the thyroid. J Pathol 169(4):465-469.

Harach HR, Wasenius VM. 1987. Expression of 'visceral' cytokeratin and ultrastructural findings in solid cell nests of the thyroid. Acta Anat (Basel) 129(4):289-292.

Hoshi N, Kusakabe T, Taylor BJ, Kimura S. 2007. Side population cells in the mouse thyroid exhibit stem/progenitor cell-like characteristics. Endocrinology 148(9):4251-4258.

Johansson E, Andersson L, Ornros J, Carlsson T, Ingeson-Carlsson C, Liang S, Dahlberg J, Jansson S, Parrillo L, Zoppoli P, Barila GO, Altschuler DL, Padula D, Lickert H, Fagman H, Nilsson M. 2015. Revising the embryonic origin of thyroid C cells in mice and humans. Development 142(20):3519-3528.

Kameda Y. 1995. Evidence to support the distal vagal ganglion as the origin of C cells of the ultimobranchial gland in the chick. J Comp Neurol 359(1):1-14.

Kameda Y. 2016. Cellular and molecular events on the development of mammalian thyroid C cells. Dev Dyn 245(3):323-341.

Kameda Y, Nishimaki T, Chisaka O, Iseki S, Sucov HM. 2007. Expression of the epithelial marker E-cadherin by thyroid C cells and their precursors during murine development. J Histochem Cytochem 55(10):1075-1088.

Lan HY, Mu W, Nikolic-Paterson DJ, Atkins RC. 1995. A novel, simple, reliable, and sensitive method for multiple immunoenzyme staining: use of microwave oven heating to block antibody crossreactivity and retrieve antigens. J Histochem Cytochem 43(1):97-102.

Lazzaro D, Price M, de Felice M, Di Lauro R. 1991. The transcription factor TTF-1 is expressed at the onset of thyroid and lung morphogenesis and in restricted regions of the foetal brain. Development 113(4):1093-1104.

Martin-Lacave I, Conde E, Moreno A, Utrilla JC, Galera-Davidson H. 1992. Evidence of the occurrence of calcitonin cells in the ultimobranchial follicle of the rat postnatal thyroid. Acta Anat (Basel) 144(2):93-96.

Martin V, Martin L, Viennet G, Challier B, Carbillet J, Fellmann D. 2000. [Solid cell nests and thyroid pathologies. Retrospective study of 1,390 thyroids]. Ann Pathol 20(3):196-201.

Matias-Guiu X. 1999. Mixed medullary and follicular carcinoma of the thyroid. On the search for its histogenesis. Am J Pathol 155(5):1413-1418.

Mizukami Y, Nonomura A, Michigishi T, Noguchi M, Hashimoto T, Nakamura S, Ishizaki T. 1994. Solid cell nests of the thyroid. A histologic and immunohistochemical study. Am J Clin Pathol 101(2):186-191.

Moreno AM, Martin-Lacave I, Montero C, Gomez-Pascual A, Fernandez A, Galera H. 1989. Demonstration of sugar residues in the ultimobranchial tubule and thyroid C-cells of the rat using peroxidase labelled lectins. Anat Histol Embryol 18(2):114-121.

Neve P, Wollman SH. 1971. Fine structure of ultimobranchial follicles in the thyroid gland of the rat. Anat Rec 171(2):259-272.

Okamoto M, Hayase S, Miyakoshi M, Murata T, Kimura S. 2013. Stem cell antigen 1-positive mesenchymal cells are the origin of follicular cells during thyroid regeneration. PLoS One 8(11):e80801.

Ozaki T, Matsubara T, Seo D, Okamoto M, Nagashima K, Sasaki Y, Hayase S, Murata T, Liao XH, Hanson J, Rodriguez-Canales J, Thorgeirsson SS, Kakudo K, Refetoff S, Kimura S. 2012. Thyroid regeneration: characterization of clear cells after partial thyroidectomy. Endocrinology 153(5):2514-2525.

Ozaki T, Nagashima K, Kusakabe T, Kakudo K, Kimura S. 2011. Development of thyroid gland and ultimobranchial body cyst is independent of p63. Lab Invest 91(1):138-146.

Preto A, Cameselle-Teijeiro J, Moldes-Boullosa J, Soares P, Cameselle-Teijeiro JF, Silva P, Reis-Filho JS, Reyes-Santias RM, Alfonsin-Barreiro N, Forteza J, Sobrinho-Simoes M. 2004. Telomerase expression and proliferative activity suggest a stem cell role for thyroid solid cell nests. Mod Pathol 17(7):819-826.

Rao-Rupanagudi S, Heywood R, Gopinath C. 1992. Age-related changes in thyroid structure and function in Sprague-Dawley rats. Vet Pathol 29(4):278-287.

Reis-Filho JS, Preto A, Soares P, Ricardo S, Cameselle-Teijeiro J, Sobrinho-Simoes M. 2003. p63 expression in solid cell nests of the thyroid: further evidence for a stem cell origin. Mod Pathol 16(1):43-48.

Rios Moreno MJ, Galera-Ruiz H, De Miguel M, Lopez MI, Illanes M, Galera-Davidson H. 2011. Inmunohistochemical profile of solid cell nest of thyroid gland. Endocr Pathol 22(1):35-39.

Suzuki K, Kobayashi Y, Katoh R, Kohn LD, Kawaoi A. 1998. Identification of thyroid transcription factor-1 in C cells and parathyroid cells. Endocrinology 139(6):3014-3017.

Takaoka M, Teranishi M, Furukawa T, Manabe S, Goto N. 1995. Age-related changes in thyroid lesions and function in F344/DuCrj rats. Exp Anim 44(1):57-62.

Thomas T, Nowka K, Lan L, Derwahl M. 2006. Expression of endoderm stem cell markers: evidence for the presence of adult stem cells in human thyroid glands. Thyroid 16(6):537-544.

Van Dyke JH. 1944. Behavior of Ultimobranchial Tissue in the postnatal Thyroid Gland: The origin of Thyroid Cistoadenomata in the rat. . Anat Rec 88:17.

Vazquez-Roman V, Utrilla JC, Fernandez-Santos JM, Conde E, Bernabe R, Sampedro C, Martin-Lacave I. 2013. Postnatal fate of the ultimobranchial remnants in the rat thyroid gland. J Morphol 274(7):725-732.

Westerlund J, Andersson L, Carlsson T, Zoppoli P, Fagman H, Nilsson M. 2008. Expression of Islet1 in thyroid development related to budding, migration, and fusion of primordia. Dev Dyn 237(12):3820-3829.

Wollman SH, Hilfer SR. 1977. Embryologic origin of various epithelial cell types in the thyroid gland of the rat. Anat Rec 189(3):467-478.

Wollman SH, Hilfer SR. 1978. Embryologic origin of the various epithelial cell types in the second kind of thyroid follicle in the C3H mouse. Anat Rec 191(1):111-121.

Wollman SH, Neve P. 1971a. Postnatal development and properties of ultimobranchial follicles in the rat thyroid. Anat Rec 171(2):247-258.

Wollman SH, Neve P. 1971b. Ultimobranchial follicles in the thyroid glands of rats and mice. Recent Prog Horm Res 27:213-234.

FIGURE LEGENDS

Figure 1. IHC profile of the different forms of UBFs appearing in rat postnatal life. A) Immature forms; B) Mature cystic UBF; C) UB cystadenomata. CK34βE12 and p63 are the most specific markers of UB remnants, which are clearly immunostained compared to the surrounding normal thyroid follicles. In contrast, immunostaining for CKAE1/AE3 or TTF-1 was also shared with the rest of the thyroid tissue. Bar: A1-B4, C3-C4=50 μm, C1-C2 = 200 μm.

Figure 2. Double immunostaining for CT and p63 in different UBFs. P63 immunopositivity (in brown) is mainly confined to the nuclei of peripheral cells in both immature (A) and mature (B) UBFs. Nevertheless, in immature forms, few scattered CT-positive cells (in red, arrows) could also be observed intermingled with p63-positive cells. Bar =50 μm.

Figure 3. Double immunostaining for Tg and p63 in immature UBFs. P63 immunopositivity (in dark blue) is located in most peripheral cells of the UBF according to a nuclear pattern. In contrast, Tg (in brown) exhibited a rather heterogeneous pattern, with scarce cells and colloid-like drops (arrow) that were immunopositive for Tg among p63-positive, Tg-negative cells (A). In panel B, one mixed follicle immunostained for Tg (arrow) could be observed merging from the UBF wall. Bar =25 μm.

Figure 4. Double IF for p63 and CT (A) and CK34βE12 and CT (B) in immature UBFs. UB remnants are strikingly immunostained for either p63 (A, in pink) or CK34βE12 (B, in red), independently as isolated cells or cell aggregates. In contrast, CT immunoreactivity (in green) was exclusively confined to C cells of the surrounding thyroid tissue. Bar =50 μm.

Figure 5. Double IF for p63 and Tg (A), and CK34βE12 and Tg (B) in immature UBFs. UB remnants are clearly immunostained for either p63 (A, in pink) or CK34βE12 (B, in red). Tg

immunoreactivity (in green) was mainly located at the colloid of normal thyroid follicles; however, some scattered positive cells were also observed forming part of the UBF wall (arrows). Furthermore, in B, a complete thyroid follicle merging, or being entrapped, from the growing UBF could be observed (asterisk). Bar=25 μm.

Figure 6. Double immunostaining for CK34βE12 and TTF-1 in serial sections of the same immature UBF. The UBF wall is clearly immunostained for CK34βE12 (cytoplasmic pattern, in red), in contrast with the surrounding negative thyroid tissue. TTF-1 immunostaining (nuclear pattern, in brown) was located in all differentiated thyroid cells as well as scarce cells within the UBF wall that coexisted (C, arrow) or not (B, arrow) with CK positivity (B). Bar =25 μm.

Table 1: Antibodies used for IHC analysis.

Antigen	Antibody	Dilution	Ag Retrieval
HMW CK	34βE12 (M, DAKO, Denmark)	RTU	H
CK AE1/AE3	M 3515 (M, DAKO, Denmark)	1:50	H
p63	4A4 (M, Santa Cruz Biotechnology, USA)	1:500	H
TTF-1	8G7G3 (M, Santa Cruz Biotechnology, USA)	1:100	H
Calcitonin	A0576 (P, DAKO, Denmark)	1:4000	-
Thyroglobulin	A0251 (P, DAKO, Denmark)	1:400	-

HMW CK, high-molecular weight cytokeratin; CK AE1/AE3, pan-keratin cocktail; TTF-1, thyroid transcription factor; M, monoclonal; P, polyclonal; RTU, Ready-To-Use; Ag, antigen; H, heating.

Table 2. Summary of the IHC Findings of UBFs and Adjacent Thyroid Endocrine Cells.

Antigens	Immature UBFs	Mature UBFs	UB Cystadenomata	C Cells	Follicular Cells
CK AE1/AE3	++	++	++	++	++
CK 34βE12	+	+	+	-	-
p63	+	+	+	-	-
TTF-1	-/+	-	-	++	++
CT	-/+	-	-	++	-
Tg	-/+	-/+	-	-	++

CK AE1/AE3, pan keratin cocktail; HMW CK, high-molecular weight cytokeratin; TTF-1, thyroid transcription factor; CT, calcitonin; Tg, thyroglobulin.
(++) = All cells and the luminal content are positive, regardless of staining intensity
(+) = Only peripheral cells show positive staining
(-/+) = Sporadic cells with positive staining
(-) = No positive cells

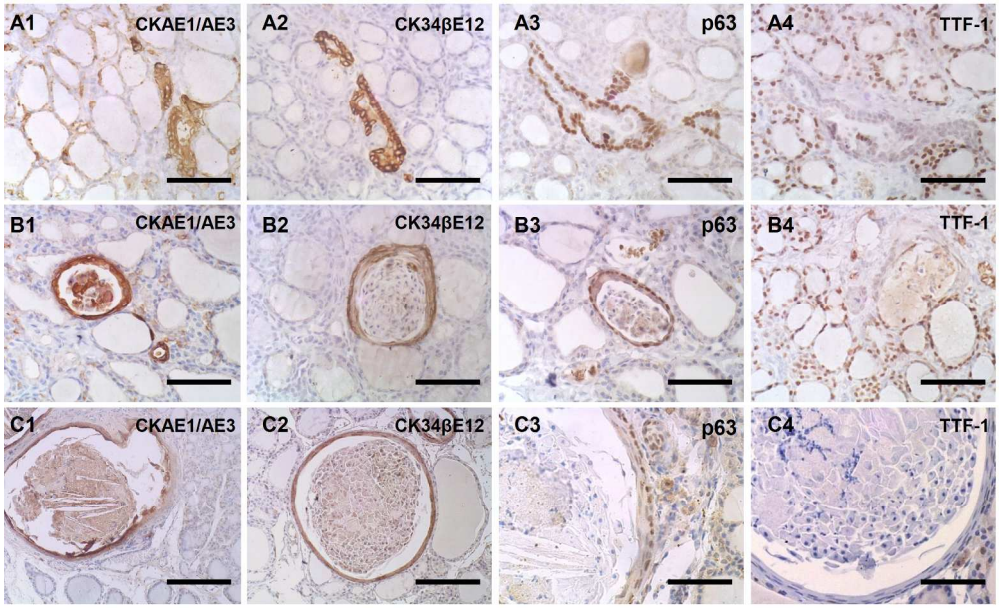

Figure 1. IHC profile of the different forms of UBFs appearing in rat postnatal life. A) Immature forms; B) Mature cystic UBF; C) UB cystadenomata. CK34βE12 and p63 are the most specific markers of UB remnants, which are clearly immunostained compared to the surrounding normal thyroid follicles. In contrast, immunostaining for CKAE1/AE3 or TTF-1 was also shared with the rest of the thyroid tissue. Bar: A1-B4, C3-C4=50 μm, C1-C2 = 200 μm.
Fig. 1
233x141mm (300 x 300 DPI)

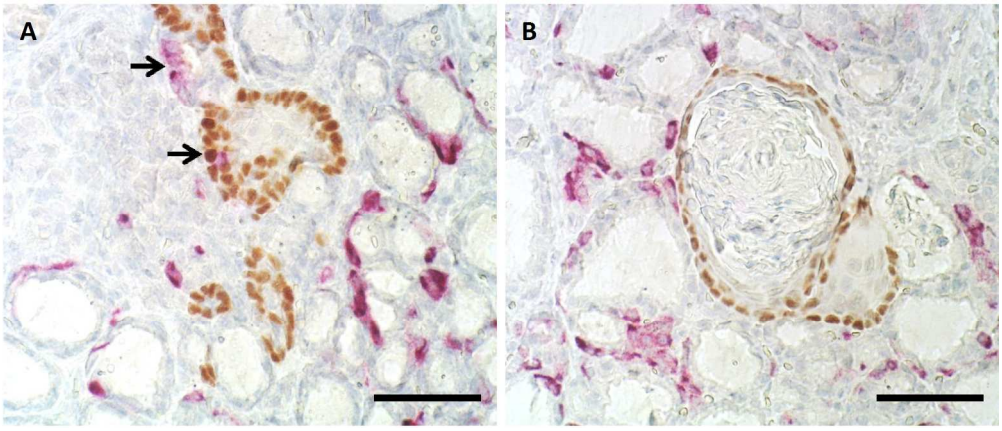

Figure 2. Double immunostaining for CT and p63 in different UBFs. P63 immunopositivity (in brown) is mainly confined to the nuclei of peripheral cells in both immature (A) and mature (B) UBFs. Nevertheless, in immature forms, few scattered CT-positive cells (in red, arrows) could also be observed intermingled with p63-positive cells. Bar =50 μm.
Fig. 2
249x106mm (300 x 300 DPI)

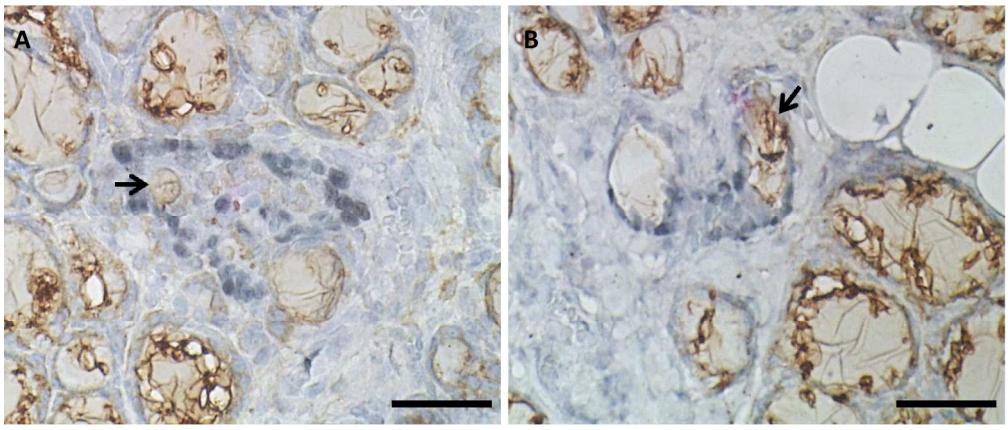

Figure 3. Double immunostaining for Tg and p63 in immature UBFs. P63 immunopositivity (in dark blue) is located in most peripheral cells of the UBF according to a nuclear pattern. In contrast, Tg (in brown) exhibited a rather heterogeneous pattern, with scarce cells and colloid-like drops (arrow) that were immunopositive for Tg among p63-positive, Tg-negative cells (A). In panel B, one mixed follicle immunostained for Tg (arrow) could be observed merging from the UBF wall. Bar =25 μm.
Fig. 3
250x105mm (300 x 300 DPI)

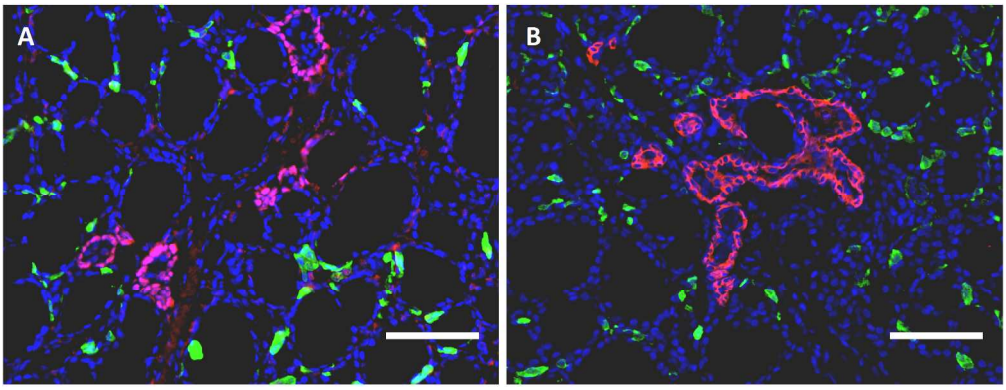

Figure 4. Double IF for p63 and CT (A) and CK34βE12 and CT (B) in immature UBFs. UB remnants are strikingly immunostained for either p63 (A, in pink) or CK34βE12 (B, in red), independently as isolated cells or cell aggregates. In contrast, CT immunoreactivity (in green) was exclusively confined to C cells of the surrounding thyroid tissue. Bar =50 μm.
Fig. 4
248x94mm (300 x 300 DPI)

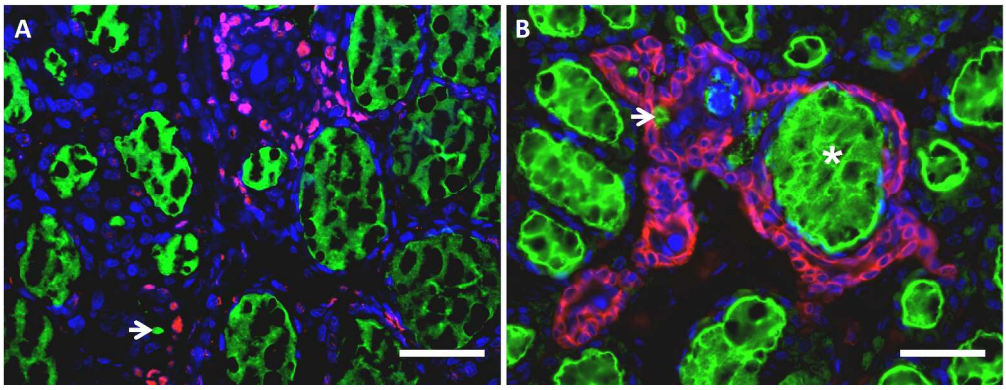

Figure 5. Double IF for p63 and Tg (A), and CK34βE12 and Tg (B) in immature UBFs. UB remnants are clearly immunostained for either p63 (A, in pink) or CK34βE12 (B, in red). Tg immunoreactivity (in green) was mainly located at the colloid of normal thyroid follicles; however, some scattered positive cells were also observed forming part of the UBF wall (arrows). Furthermore, in B, a complete thyroid follicle merging, or being entrapped, from the growing UBF could be observed (asterisk). Bar=25 μm.
Fig. 5
248x94mm (300 x 300 DPI)

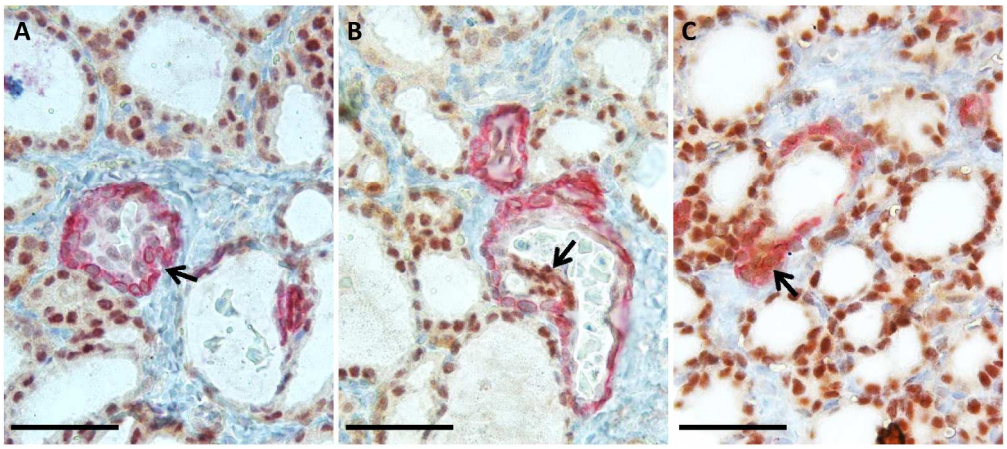

Figure 6. Double immunostaining for CK34βE12 and TTF-1 in serial sections of the same immature UBF. The UBF wall is clearly immunostained for CK34βE12 (cytoplasmic pattern, in red), in contrast with the surrounding negative thyroid tissue. TTF-1 immunostaining (nuclear pattern, in brown) was located in all differentiated thyroid cells as well as scarce cells within the UBF wall that coexisted (C, arrow) or not (B, arrow) with CK positivity (B). Bar =25 μm.
Fig. 6
248x109mm (300 x 300 DPI)